Journal of Academic Research in Multidisciplinary Studies
Vol: 02; **Issue:** 01; Jan-Jun 2025; **Pg:** 013-021

Long-Term Crack Healing and Durability Enhancement of UHPC under Sustained Load in Harsh Environments

Santosh Kumar Gayakwad
Professor, Department of Computer Science, Managalayatan University, Hubli, Karnataka, India
Email Id: iksantosh01@gmail.com

Received: 04th February 2025 / Accepted: 21th February 2025 / Published: 17th March 2025

Citation: Santosh Kumar Gayakwad (2024). Long-Term Crack Healing and Durability Enhancement of UHPC under Sustained Load in Harsh Environments, Journal of Academic Research in Multidisciplinary Studies, 1(1), 013-021
DOI: https://doi.org/10.54646/jarms.2025.03

Abstract: Durability enhancement in Ultra-High-Performance Concrete (UHPC) is of growing interest due to its application in aggressive environments such as saline and geothermal conditions. This study investigates the self-healing performance of pre-cracked UHPC under sustained tensile stress when exposed to tap water, saltwater, and geothermal water for up to 12 months. The healing behavior was assessed using crack self-sealing index (ICS), ultrasonic pulse velocity (UPV), stiffness recovery index (ISR), chloride penetration resistance, and SEM/EDS analysis of healing products. Results show that narrow cracks (0.1 mm) healed faster and more completely than wider cracks (0.3 mm). Tap water promoted the most efficient healing, achieving 100% crack closure within three months, whereas saltwater and geothermal water required longer exposure, with partial inhibition caused by chloride and sulfate ions. Nonetheless, prolonged immersion allowed significant sealing, stiffness recovery of 20–40%, and reduced chloride penetration. SEM confirmed calcium carbonate as the main healing product, with higher crystallinity in tap water. The findings highlight UHPC's robust self-healing ability even under harsh environments, though long-term field validation and studies on variable crack dynamics remain necessary.
Keywords: *Ultra-High-Performance Concrete (UHPC); Sel healing; Load effect*

INTRODUCTION

These days, the building and civil engineering sectors prioritize long-term viability and environmental friendliness. They affect maintenance costs and the lifespan of buildings directly [1,2]. Due to its brittle nature, concrete easily breaks under tensile stresses, which compromises its durability. For example, concrete buildings near the coast could crack and spall due to chemical penetration and corrosion of reinforcement caused by saltwater.

A new set of structural problems is emerging with the growing popularity of renewable energy sources. In areas like central and southern Italy, where infrastructure is vital for tapping into geothermal energy supplies, the corrosion of cementitious materials caused by geothermal water becomes a major worry [3]. The harsh conditions caused by the high sulfate ion content of the geothermal water decrease the structure's performance and safety, raise the expense of repairs and maintenance, and even cause the building to collapse. Consequently, there has been a lot of buzz about finding longer-lasting materials and ways to enhance concrete's performance to keep cracks at bay and chemical attacks at bay. In order to consistently consider the real benefits of these sophisticated materials, it is necessary to create and validate performance-based durability design approaches. In order to effectively handle these difficulties, structural design standards must move away from the existing "deemed to satisfy" prescriptive techniques that rely on material composition.

Uniquely created from a combination of cement, fibers, and tiny particles, UHPC is a composite material with exceptional performance qualities. This material's strong compressive strength, tensile deformation, and energy dissipation capabilities are all results of its very well-designed dense internal structure and outstanding mechanical qualities. After 28 days, UHPC has the potential to surpass ordinary concrete's compressive strengths of 150 MPa, as per ACI Committee 239. The tensile strain hardening response is characterized by UHPC's tensile strength ranging from 8 to 10 MPa and a tensile strain capacity more than 0.2% (the yield strain of steel) when fibers are suitably doped into the material [4]. Fracture width in usage phase settings is limited to 0.02-0.03 mm due to the continuous recurrent cracking of UHPC [5].

A denser inner structure is one reason why UHPC has a longer lifetime, according to research [6]. Mechanical stresses, swings in humidity and temperature, shrinkage, creep deformation, and environmental impacts like chemical attacks can cause cracks in concrete when it is placed in service. Concrete will crack over time, regardless of UHPC. Damage to UHPC from exposure to harsh conditions can accelerate degradation of the cement matrix and fiber reinforcement. These fissures might allow potentially dangerous ions to enter the body. This means UHPC might degrade significantly and lose some of its original material properties, making it less effective at achieving its high-performance goals. While there has been little investigation into the factors that affect UHPC's long-term durability, the performance of fractured UHPC under situations of prolonged stress remains mostly unknown [7,8]. The ability of UHPC to retain its tensile capabilities over time is a key differentiator from conventional (reinforced) concrete, which sometimes ignores these attributes while being designed. Tensile properties are one of the many design criteria utilized in UHPC applications. Preserving these characteristics is crucial for the structure's projected structural service conditions and its ability to endure for its intended service life. Another important trait that impacts UHPC's lifespan is its capacity to fix itself. Autogenous self-healing is an inherent property of UHPC because to its low water-cement ratio. The self-healing process of UHPC is activated when water penetrates the material. This mechanism then produces molecules that bind the cracks. There will be less hostile foreign media able to get in thanks to this method. In addition, UHPC has used certain "stimulating" self-healing procedures to help the material's natural healing properties, so they can fix broken areas [9]. According to Ahn et al. (2012) [10], UHPC was made using 20% fly ash (FA), 7% silica fume (SF), and 26% water to binder (w/b). The restorative materials proved they could seal cracks smaller than 100 μm after being immersed in water for seven days. Wang et al. (2022) [11] tested UHPC samples with and without SCEA, or expansive agents based on silicate-modified calcium oxide, using a water-to- binder ratio of 0.2. The crack width significantly decreased from 180 μm to 70 μm in the samples treated with SCEA. Lo Monte and Ferrara (2021) [12] stated that after six months of exposure to water, UHPC samples containing slag showed better recovery in bending performance. It was determined that this improvement was due to the fact that the hydration activities of the slag particles expanded with time.

Objective of study

A self-healing characteristic of pre-cracked UHPC renders it resistant to mechanical stress and wear and tear, as per the research. Moreover, it offers a framework for modeling real-world structural service in order to assess the self-healing capabilities of materials composed of cement. Conducting this kind of testing is essential for incorporating self-healing into design ideas and performance-based verification approaches.

METHODOLOGY

The UHPC mix proportions used in this study are displayed in Table 1.1. To achieve a dense and robust matrix, the weight-to-binder ratio of CEMI and slag was 0.18. “Penetron Admix (R)”, a crystalline admixture, was used as a healing stimulant at a concentration of 0.8% by weight. An efficient way to increase concrete's healing capacity is to add crystalline additive. Use of 1.5% volume of straight steel fibers “(Azichem Readymesh MR 200 (R))” with dimensions of $\boldsymbol{l_f = 20\ mm}$ and $\boldsymbol{d_f = 0.22\ mm}$ enhanced the tensile hardening properties. The composition of the mix and the pouring process are further described in previous studies.

While the material was still in the production, the slabs utilized for the trials were cut. For a year, the slag was maintained in a controlled laboratory environment with relative humidity of 90% and temperature of 20 degrees Celsius to mitigate the effect of late hydration on the evaluation of its self-healing capacity. Careful shaping of square specimens cut from thin plates made up the DEWS samples. You may see the DEWS form in Figure 1.1. Refer to Cuenca et al. (2021) [13] for further information on the thickness, which is 30 mm. A well-established indirect tensile test technique, the DEWS test can determine the constitutive connection between COD and tensile stress. In contrast to other methods for deducing the tensile constitutive relationship from bending test data, this one is straightforward and doesn't need back analysis.

The pre-cracking of the DEWS samples was deliberate. Two LVDTs were placed on each side of the sample to track its displacement, as seen in Figure 1.2. For small cracks, a COD value of 0.1 mm was ideal, while for larger ones, a value of 0.3 mm. The choice of COD to enable future comparative investigations was based on prior research. Upon reaching the specified average COD value—approximately 0.1 mm/0.3 mm—t
he loading procedure was stopped and the highest force was recorded.

In Figure 1.3, we can see the results of applying continuous through-crack tensile stress to the pre-cracked DEWS specimens using a proprietary load-holding apparatus. Nuts, two 100 mm steel bars with a diameter of 10 mm, four interchangeable metal plates with dimensions of 15x 15x15cm, and four bolts make up the device. The nuts at the bottom became snugger while the ones at the top became looser. Following this, identical to the pre-cracking test, the sample was subjected to compressive loading. At the target COD value, the load was exactly proportional to the force that the sample felt just before it broke. Until the target load was reached, the operator steadily applied compression force by pressing the "hold" button on the machine's control panel. The bolts were driven through once the force had been transferred to the metal plates. The control panel displayed a decrease in load, and the force was redirected to the specimen through the plates and bars following an adjustment of the top nuts on the bolts. We locked the instrument and filled the specimen to capacity after the readings fell to zero.

Table 1. Mixture Design (UHPC)

Material (kg/m^3)	Cement (CEM I 52.5R)	Slag	Water	Fibers (steel)	Fine aggregate (0 – 2 mm)	Superplasticizer	Crystalline agent
Value	600	500	200	120	982	33	4.8

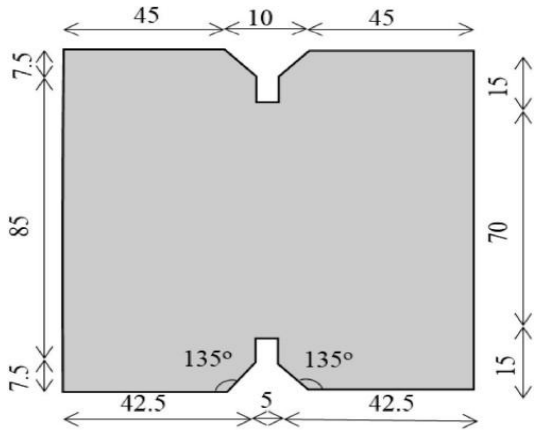

Figure 1. Configuration and measurements of DEWS specimens

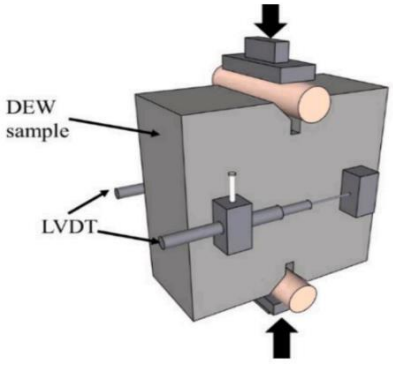

Figure 2. Configuration of DEWS testing platforms.

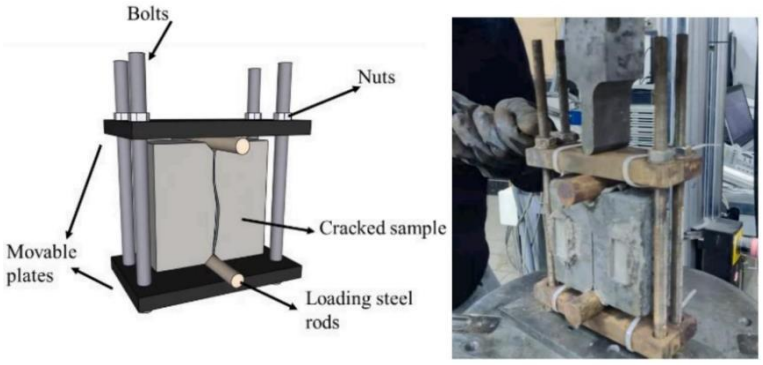

Figure 3. Test apparatus for prolonged loading of DEWS specimens.

It just took five to ten minutes to finish the re-loading testing process after placing the shattered specimen in the device's center. In keeping with earlier remarks, the samples were "submitted" to the continuing load. Water from the tap, water with a 3.3% salt concentration, and water from a reservoir in the cooling tower of a geothermal power plant were the three different situations that the individuals were then put through. High concentrations of chlorides and sulphates were found in the geothermal water, which was tested in three different settings for different durations using cracked and uncracked reference samples: one month, three months, six months, and twelve months. The evolution of the self-healing capabilities might be tracked in this way. Each functional condition uses two samples. Case in point: two samples maintained a COD of 0.1 mm after three months in water.

The "DinoLite digital optical microscope and its accompanying software, DinoLite Capture," were used to look for signs of fracture closure in the samples. Each picture only caught a little portion of the crack, so to reproduce it in its entirety, we used Photoshop to combine many images of the same fissure. Images were taken using a digital microscope both before and after each recovery period. We used Photoshop's measurement tool to find the cracked length, l_{crack} , and the magic wand tool to choose and quantity the rebuilt crack area, , A_{crack} , Dividing A_{crack} by l_{crack} } is one approach to determining the average crack width, W. The self-healing capability was evaluated by developing and computing an index of crack self-sealing (ICS) using Eq. (1.1).

$$\text{Index of crack self sealing } = \frac{W_{\text{initial}} - W_{\text{after sealing}}}{W_{\text{initial}}} \ldots\ldots\ldots\ldots (1.1)$$

the initial crack width is denoted as w_{initial} and the crack width after sealing is denoted as $w_{\text{after sealing}}$

The first step after the re-loading test was to determine the initial crack widths. Figure 1.4 displays the crack width distribution for samples under various conditions.

The UPV test is a well-known and respected way to find out whether concrete can self-heal and is durable. In Fig. 1.5, we can see the UPV test's fundamental operational idea. Use of an emitter and a receiver embedded in concrete allows for the estimation of sound wave velocities using this method. Depending on the width and depth of the same fracture, the speed of these waves changes as they move over a discontinuity, such as a split in concrete. All of the tests in this investigation used a 100 mm spacing between the transmitter and receiver. A 50 mm transducer operating at 50 kHz was used for the test. Intact, pre-cracked, and unloaded sealed DWES samples were the three different kinds of samples that were subjected to the UPV testing. The wave velocities were calculated by monitoring how long it took for the waves to pass through the sample. To compare the sound wave velocities in the intact, pre-cracked, and sealed samples, the suggested index of velocity recovery (IVR) is shown in Equation (1.2). This will allow us to evaluate the extent of the harm and how well the body's own healing mechanisms are functioning.

$$IVR = \frac{UPV_i}{UPV_{\text{intact}}} \ldots\ldots (1.2)$$

and the velocity of the intact sample is denoted as UPV_{intact} whereas the velocity of the crack sample is represented by UPV_i in the i-th period.

After1,3,6, and 12 months of exposure, the loaded samples were taken out of the loading device and put through a final splitting tensile test to examine the mechanical property recovery of pre-cracked UHPC samples in various exposure conditions. To ensure that the specimens failed entirely, they were loaded at the same rate as in the pre-cracking testing. Eq. (1.3) calculates the Index of Stiffness Recovery (ISR) from the stress vs. crack open displacement curves. Figure 1.6 illustrates this calculating principle.

$$ISR_0 = \frac{K_c^f - K_u^0}{K_c^0 - K_u^0} \quad \text{.....(1.3)}$$

where K_c^0 represents the initial loading stiffness, K_u^0 stands for the unloading stiffness, and K_c^f denotes the ultimate loading stiffness following the exposure time setting.After the last round of failure testing, samples were sprayed with silver nitrate to see if they could withstand chloride penetration in saltwater. As a treatment, a 0.1 mol/L AgNO3 solution

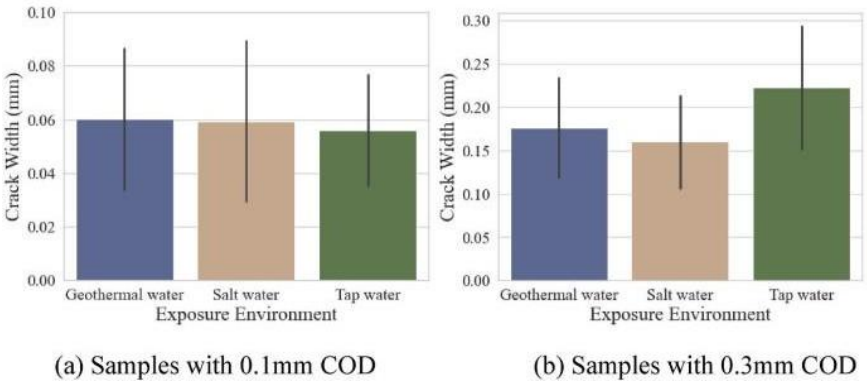

Figure 4. Crack width profile after reloading (error bars = standard deviation)

was sprayed over the fracture surfaces of the newly divided DEWS samples. Whereas areas polluted with chloride became white or light gray, areas uncontaminated with chloride became a pale brown [13]. The parts that were titrated were photographed using an optical microscope. To determine the amount of chloride penetration and to create the color shift border, the photographs were edited in Photoshop.

Figure 5. UPV Representation.

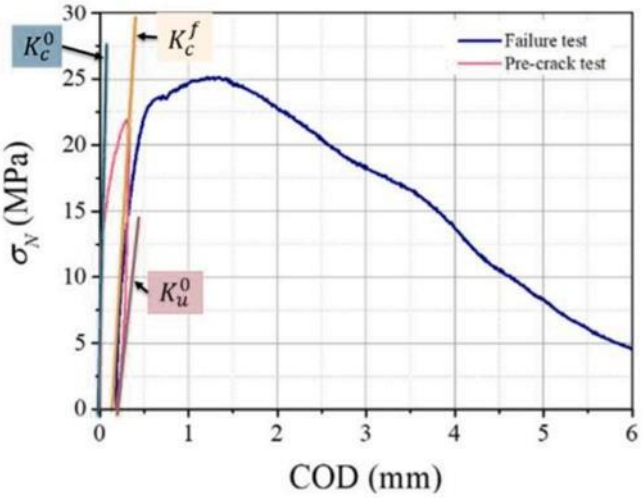

Figure 6. Resilience index

An SEM was used to examine the morphological and microstructural alterations of UHPC self-healing products that were subjected to different conditions. The specimens were analyzed using scanning electron microscopy (SEM) after three and six months of exposure to various conditions. The area around the DEWS samples that did not pass the final splitting test was collected in order to provide test samples with dimensions of 10x10x10 mm. To capture the SEM images, the equipment was set up in high vacuum mode with a variable working distance and an accelerating voltage of 20 kV. Energy dispersive X-ray spectroscopy (EDS) and scanning electron microscopy (SEM) were also employed to determine the distribution of the healing product's primary components.

RESULTS

The performance of pre-cracked UHPC specimens exposed to various water environments under sustained load was studied using various characterization techniques. These techniques included SEM/EDS analysis of healing products, chloride penetration resistance, Index of Stiffness Recovery (ISR), UPV, and Index of Crack Self-Sealing (ICS). All things considered, the results of these tests provide light on UHPC's self-healing capabilities and its resilience in the face of violent exposure. The findings are integratedly discussed in the following subsections, with a focus on the role of crack width, exposure medium, and healing length.

Crack Closure and Self-Sealing (ICS)

The evolution of crack widths was monitored in specimens with initial crack opening displacements (COD) of 0.1 mm (narrow) and 0.3 mm (wide). Results revealed a clear dependency of healing efficiency on crack width and exposure environment. Narrow cracks demonstrated superior healing, closing almost entirely within shorter timeframes. In tap water, cracks of 0.1 mm achieved complete closure within three months, with the ICS value reaching 100%. Saltwater exposure delayed complete sealing to six months, while geothermal water further slowed the process, achieving around 97% closure even after one year. Wider cracks also healed effectively, though at a reduced rate. After 12 months, ICS values for 0.3 mm cracks reached 100% in saltwater and approximately 85% in geothermal water.
The results show that the UHPC can withstand the effects of harsh conditions, such seawater and geothermal water, after prolonged exposure. This shows that, especially in more dangerous settings, time is of the essence for full recovery.

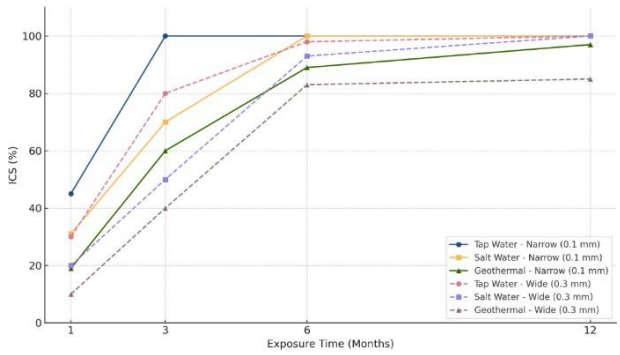

Figure 7. Index of Crack Self-Sealing (ICS) over Time

Healing Efficiency through Ultrasonic Pulse Velocity (UPV)

UPV measurements complemented ICS by quantifying internal crack closure and microstructural restoration. The Index of Velocity Recovery (IVR) increased progressively with exposure time, with 0.1 mm cracks exhibiting the most pronounced recovery. In tap water, IVR values for narrow cracks reached unity within six months, indicating nearly complete healing. Wider cracks in the same environment achieved near-complete recovery after 12 months. Saltwater and geothermal water slowed the healing process, but even in these aggressive media, IVR values approached 0.95–0.99 by the end of the year.
These results are consistent with ICS trends, confirming that water penetration triggers delayed hydration and precipitation reactions within the cracks, thereby enhancing structural restoration. Narrow cracks, which provide a more favorable geometry for deposition, showed consistently better healing rates.

Mechanical Recovery and Stiffness Retention (ISR)

Mechanical property recovery was assessed using the Index of Stiffness Recovery (ISR), derived from stress–COD curves in post-exposure splitting tests. Results showed a gradual improvement in stiffness over time, further verifying that self-healing not only sealed cracks but also restored load-bearing capacity. Narrow cracks consistently demonstrated higher ISR values than wider cracks. After one month, stiffness recovery ranged between 12–17%, depending on the environment. With prolonged exposure, ISR values reached 39% in tap water, 38% in saltwater, and 36% in geothermal water after 12 months.

Although the absolute differences between environments narrowed with time, the rate of recovery decreased after six months. This deceleration is attributed to reduced availability of reactive compounds and limited ingress of water once cracks had partially sealed. Nevertheless, no mechanical degradation was observed even in aggressive environments, demonstrating the robustness of UHPC under sustained stress.

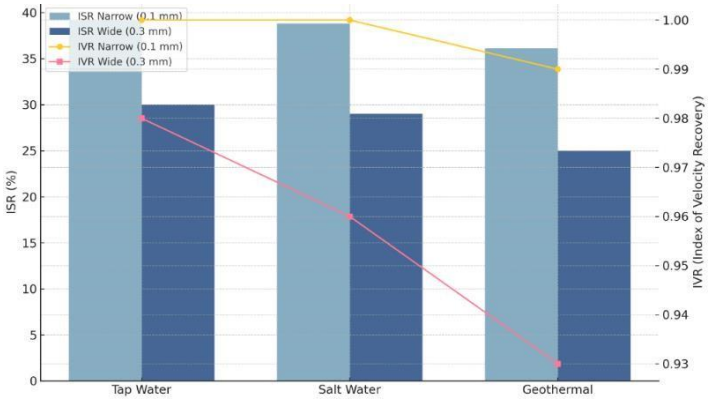

Figure 8. Mechanical Recovery (ISR) and Healing Efficiency (IVR) after 12 Months

Resistance to Chloride Penetration

Saltwater exposure was used to assess the resistance of self-healed cracks to chloride ingress. Results from $AgNO_3$ spray tests showed that chloride penetration velocity decreased significantly with healing duration. Narrow cracks reduced penetration depth more

effectively than wide cracks, demonstrating the critical role of geometry in mitigating ionic diffusion. After 12 months, penetration rates for both crack sizes had decreased substantially, largely due to complete or near-complete crack closure. Interestingly, the relative difference in chloride ingress between 0.1 mm and 0.3 mm cracks also diminished over time, suggesting that extended exposure allowed wider cracks to achieve sufficient sealing to resist aggressive ion transport.

These findings reinforce the protective role of self-healing in enhancing the durability of UHPC, particularly in marine or saline environments.

Morphology of Healing Products (SEM/EDS Analysis)

Microstructural characterization via SEM and EDS confirmed the formation of healing products within cracks across all environments. The predominant compound was calcium carbonate ($CaCO_3$), with morphology and crystallinity influenced by the exposure medium. In tap water, abundant polyhedral calcite crystals were observed, indicating stable and well-formed deposits. This explains the superior healing performance in this medium. Saltwater and geothermal water, however, reduced crystallization rates due to the presence of chloride and sulfate ions, respectively. These ions hindered calcite growth and produced less well-defined morphologies.

Nonetheless, prolonged exposure allowed significant deposition to occur, even in aggressive environments. Healing products often accumulated at the fibre–matrix interface, enhancing bond strength and improving stiffness recovery. This dual role of crack sealing and fibre–matrix reinforcement highlights the multifunctional benefits of self-healing mechanisms in UHPC.

DISCUSSION OF RESULTS

The combined results from ICS, UPV, ISR, chloride penetration, and SEM analyses converge on several key findings. First, crack width is the most decisive factor influencing healing rate: narrower cracks not only heal faster but also show better mechanical recovery and chloride resistance. Second, exposure medium significantly affects kinetics, with tap water offering the most favorable environment, while geothermal water is the most challenging due to its sulfate and chloride content. Third, while aggressive environments delay healing, they do not prevent it; extended exposure compensates for early limitations, allowing eventual near-complete recovery. Finally, the deposition of $CaCO_3$ and the strengthening of fibre–matrix bonds provide a mechanistic explanation for observed stiffness recovery and durability enhancement.

CONCLUSIONS

In this study, we tested UHPC's self-healing capabilities in modern weather and long-term mechanical stresses. In order to verify the effect of environmental exposure and continuous tensile stresses on UHPC through cracks, the researchers built and established a sustained load system. To track how UHPC's self-healing capabilities have developed, we used a suite of tests and evaluation metrics. Based on the investigation, the following results were reached that the ability to cure oneself is greatly improved by prolonged exposure. Municipal water sources are more effective as a therapeutic resource than samples of saltwater or geothermal water. Full closure (100 % ICS) is commonly achieved by submerged fractures in three months or less. While geothermal water normally reaches 89% ICS after six months, saltwater usually reaches 100%. The amount and rate of self-healing are significantly affected by how humid an atmosphere is. Submerging the damaged area in saltwater for 12 months and geothermal water for 85.1 months may counteract the inhibiting effects of unfavorable circumstances on self-healing. A total ICS of 100% and an ICS of 85.1% are the outcomes of this. There was a steady but slow rise in the IVR. However, recovery periods were slower for seawater and geothermal samples, suggesting that the fissures were not fully filled. These assertions are supported by the findings of the ICS investigation. Stiffness is regaining its previous level even when loading remains constant, as shown by increasing ISR readings.The self-healing process of the UHPC restores its mechanical characteristics twelve months after the fracture occurs, leading to a twenty to forty percent increase in overall stiffness. The ISR readings were greater in the 0.1 mm COD samples compared to the 0.3 mm COD samples. Samples exposed to saltwater or geothermal water recovered their mechanical properties less well than those exposed to tap water. After one year, samples treated with 0.1 mm COD showed no noticeable change in ISR. Prolonged exposure did raise ISR, although at a far slower rate. Fourthly, spray testing with an AgNO3 solution showed that longer exposure periods and bigger cracks allowed chloride ions to penetrate deeper. On the other hand, when the exposure time grew, the penetration rate dropped dramatically. The key reason for this decrease was the presence of self- healing fissures, which prevented further chloride ions from entering. No matter the setting, scanning electron microscopy and energy dispersive spectroscopy revealed that CaCO3 was the principal ingredient in the samples' self-healing goods. The presence of more polyhedral calcite-characterized CaCO3 crystals on the fiber surfaces suggests that the crystallinity level was higher in the tap water. After three months of exposure to salt and geothermal water, the rate of CaCO3 crystallization was shown to be slowed down as a result of the effects of chloride and sulfate ions. There were still many polyhedral CaCO3 crystals visible six months following exposure. Any possible decreases induced by the intense exposure environment were more than compensated for by the continual healing process and extended exposure.

REFERENCE

1. [1] H. Van Damme, Concrete material science: past, present, and future innovations, Cement Concrete Residual. 112 (2018) 5–24
2. [2] H. Beushausen, R. Torrent, M.G. Alexander, Performance-based approaches for concrete durability: state of the art and future research needs, Cement Concr. Res. 119 (2019) 11–20
3. [3] S. Al-Obaidi, P. Bamonte, F. Animato, F. Lo Monte, I. Mazzantini, M. Luchini, S. Scalari, L. Ferrara, Innovative design concept of cooling water tanks/basins in geothermal power plants using ultra-high-performance fiber-reinforced concrete with enhanced durability, Sustainability 13 (2021) 9826
4. [4] I.L. Larsen, R.T. Thorstensen, The influence of steel fibres on compressive and tensile strength of ultra-high-performance concrete: a review, Construct. Build. Mater. 256 (2020), 119459
5. [5] L. Teng, H. Huang, K.H. Khayat, X. Gao, Simplified analytical model to assess key factors influenced by fiber alignment and their effect on tensile performance of UHPC, Cem. Concr. Compos. 127 (2022), 104395

6. [6] S. Al-Obaidi, M. Davolio, F. Lo Monte, F. Costanzi, M. Luchini, P. Bamonte, L. Ferrara, Structural validation of geothermal water basins constructed with durability enhanced ultra high performance fiber reinforced concrete (Ultra High Durability Concrete), Case Stud. Constr. Mater. 17 (2022), e01202
7. [7] M. Amran, S.S. Huang, A.M. Onaizi, N. Makul, H.S. Abdelgader, T. Ozbakkaloglu, Recent trends in ultra-high performance concrete (UHPC): current status, challenges, and future prospects, Construct. Build. Mater. (2022)
8. [8] J. Du, W. Meng, K.H. Khayat, Y. Bao, P. Guo, Z. Lyu, A. Abu-obeidah, H. Nassif, H. Wang, New development of ultra-high-performance concrete (UHPC), Composites, Part B 224 (2021), 109220
9. [9] B. Xi, S. Al-Obaidi, L. Ferrara, Effect of different environments on the self-healing performance of Ultra High-Performance Concrete – a systematic literature review, Construct. Build. Mater. 374 (2023), 130946
10. [10] T.H. Ahn, D.J. Kim, S.H. Kang, Crack self-healing behavior of high performance fiber reinforced cement composites under various environmental conditions, in: Earth Sp. 2012 - Proc. 13th ASCE Aerosp. Div. Conf. 5th NASA/ASCE Work. Granul. Mater. Sp. Explor., 2012
11. [11] Y.-S. Wang, H.-S. Lee, R.-S. Lin, X.-Y. Wang, Effect of silicate-modified calcium oxide-based expansive agent on engineering properties and self-healing of ultrahigh-strength concrete, J. Build. Eng. 50 (2022), 104230
12. [12] F. Lo Monte, L. Ferrara, Self-healing characterization of UHPFRCC with crystalline admixture: experimental assessment via multi-test/multi-parameter approach, Construct. Build. Mater. 283 (2021), 122579
13. [13] E. Cuenca, L. D'Ambrosio, D. Lizunov, A. Tretjakov, O. Volobujeva, L. Ferrara, Mechanical properties and self - healing capacity of ultra high performance fibre reinforced concrete with alumina nano-fibres: tailoring ultra high durability concrete for aggressive exposure scenarios, Cem. Concr. Compos. 118 (2021), 103956